THE JOURNAL OF NAVIGATION (2019), **72**, 193–206.
doi:10.1017/S0373463318000590

A Passive Acoustic Positioning Algorithm Based on Virtual Long Baseline Matrix Window

Tao Zhang, Ziqiang Wang, Yao Li and Jinwu Tong

(*Southeast University, Nanjing, School of Instrument Science and Engineering, Key Laboratory of Micro-Inertial Instrument and Advanced Navigation Technology of Ministry of Education, Nanjing 210096, China*)
(E-mail: 101011356@seu.edu.cn)

A new acoustic positioning method for Autonomous Underwater Vehicles (AUV) that uses a single underwater hydrophone is proposed in this paper to solve problems of Long Baseline (LBL) array laying and communication synchronisation problems among all hydrophones in the traditional method. The proposed system comprises a Strapdown Inertial Navigation System (SINS), a single hydrophone installed at the bottom of the AUV and a single underwater sound source that emits signals periodically. A matrix of several virtual hydrophones is formed with the movement of the AUV. In every virtual LBL window, the time difference from the transmitted sound source to each virtual hydrophone is obtained by means of a Smooth Coherent Transformation (SCOT) weighting cross-correlation in the frequency domain. Then, the recent location of the AUV can be calculated. Simulation results indicate that the proposed method can effectively compensate for the position error of SINS. Thus, the positioning accuracy can be confined to 2 m, and the method achieves good applicability. Compared with traditional underwater acoustic positioning systems, the proposed method can provide great convenience in engineering implementation and can reduce costs.

KEYWORDS

1. Single sound source positioning. 2. Inertial navigation system. 3. Virtual LBL matrix window. 4. COT weighting cross-correlation in frequency domain.

Submitted: 15 March 2018. Accepted: 9 July 2018. First published online: 2 August 2018.

1. INTRODUCTION. Autonomous Underwater Vehicles (AUVs) play important roles in ocean pollution monitoring and seabed, marine mineral and oil resources investigation due to their advantages, which include unmanned operation, the capability to enter narrow underwater environments and relatively low cost (Choi et al., 2015; Ji et al., 2014; Yu and Wu, 2015; Zhong et al., 2015).

Highly accurate underwater navigation and positioning technologies are required for AUVs to accomplish these missions (Zhang et al., 2013). In terms of current navigation technologies, integrated navigation systems of underwater acoustic and Inertial Navigation Systems (INSs) are widely used for AUVs (Zhang et al., 2016b). Although INSs have

autonomous characteristics and are useful when concealment is required, their errors increase with time and limit their continuity (Morgado et al., 2010). To achieve a high positioning precision over longer periods, INSs are required to use other external information to periodically correct the position errors during navigation (Paull et al., 2014; Deng et al., 2009; Mahdinejad and Seghaleh, 2013). Global Navigation Satellite Systems (GNSS) and other radio signals cannot be used underwater due to their rapid attenuation that requires AUVs to float toward the water surface to receive satellite signals for positioning (Jiao et al., 2013; An et al., 2013; Barisic et al., 2012). These conditions seriously reduce system efficiency, expose the current position of AUVs and influence the real-time characteristics of information interaction. Therefore, accurate navigation technologies are key factors in AUV development (Ferreira et al., 2010).

Compared with electromagnetic waves, the attenuation rate of sound waves in the ocean is low so that they can spread over long distances (Ngatini et al., 2016). Long baseline positioning methods are used worldwide. Paull et al. (2014) summarised the recent advances of underwater vehicle navigation and positioning and introduced several traditional methods (Ji et al., 2016). Donovan (2012) adopted integrated tests and a real-time terrain particle filter framework to complete the positioning and navigation of AUVs. Lee et al. (2005) optimised the number of transponders that simplified the matrix model. Maki et al. (2013) proposed a method that estimates the position and direction of underwater vehicles by using a single bottom station without expensive INSs or time-consuming calibration. Miller et al. (2010) established a type of positioning system using a tight LBL/Doppler Velocity Log (DVL)/INS integration method, which is suitable for AUV positioning in a complicated deep sea environment. These studies proposed several valuable solutions that were based on long baseline systems and promoted the application of underwater acoustic positioning worldwide.

However, several limitations of Long Baselines (LBL) were reported in the literature. Zhang (2016a) indicated a series of engineering implementation problems, such as the number of transponders being so large that they complicated the matrix system and made the laying, calibrating and recalling processes tedious. Casalino et al. (2014) used buoys rather than traditional seabed transponders. However, several instability errors were introduced in this method because the positions of the buoys were unfixed and the buoys thus floated in the sea; in addition, their positions were frequently calibrated, leading to increased workload. In Zhang et al. (2015), acoustic signals were received from different transponders at different periods, and a synchronising technology was required before processing all the signals from different transponders. In addition, the method mentioned in Zhang et al. (2015) allowed AUVs to be easily monitored by others and reduced their concealment.

To solve these problems, we have designed a passive acoustic positioning method based on a virtual LBL matrix window algorithm that uses a single sound source. This method does not require AUVs to float toward the surface to update their location and offers high concealment and safety. This method also reduces the difficulty in releasing transponders because only one sound source is placed at the bottom of the sea and one hydrophone is installed at the bottom of the AUV. In addition, all received signals can be directly processed by the computer embedded in the AUV without time synchronisation and then returned to the AUV for processing. Thus, the complexity and cost are significantly reduced. Moreover, the virtual LBL matrix window method can be used to estimate AUV position through a few time windows. This method does not require a large number of data points and guarantees a good real-time performance. The accuracy increases with the

https://doi.org/10.1017/S0373463318000590 Published online by Cambridge University Press

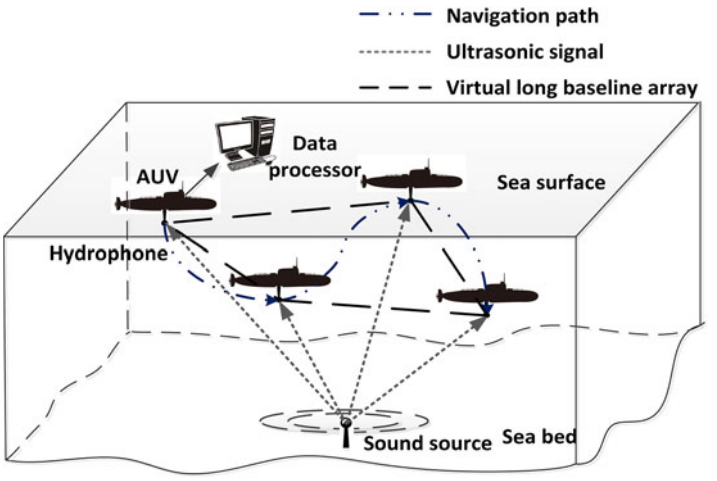

Figure 1. Formation of virtual LBL matrix.

number of iterations of the matrix window. Therefore, this method provides a new concept for AUV positioning.

2. SYSTEM PRINCIPLE AND STRUCTURE.

2.1. *Formation of virtual LBL matrix window.* The proposed method in this study is based on a virtual LBL matrix window. In this system, a single sound source is placed at the bottom of the sea and sends periodic signals and a single hydrophone is installed on the AUV. In the AUV navigation trajectory, four selected recent positions of the AUV are regarded as four virtual hydrophones of the LBL matrix, which constitute a virtual LBL matrix window, as shown in Figure 1.

2.2. *Positioning algorithm based on a moving virtual LBL matrix window.* In this method, the single sound source is fixed on the seabed in which its absolute position is measured as (x, y, z) in advance in Earth-centred Earth-fixed coordinates. This sound source sends periodic pulse signals at regular intervals, with the time period defined as *Ts*. A virtual LBL matrix window is created when the AUV enters the area where the source signal can be received. The current position of the AUV is set as the initial position P_0, where the period of receiving acoustic signals is denoted as x_0. Then, the AUV continues to move forward, and its position is denoted as P_1 at the beginning of the eleventh period. A period of receiving acoustic signals is denoted as x_1. In this way, the AUV position is denoted as $P_i(i = 2, 3, \cdots)$, and the receiving acoustic signal is denoted as $x_i(i = 2, 3, \cdots)$ for every ten periods. Each of the four consecutive positions of the AUV forms a virtual LBL matrix window. For example, the first virtual LBL matrix window is composed of the initial four positions (P_0, P_1, P_2, P_3), which are marked by the blue rectangle in Figure 2. The second virtual LBL window is formed by removing position P_0 and adding position P_4 when the AUV arrives at position P_4; this window is shown as the red rectangle in Figure 2. In this way, the moving virtual LBL windows are established by removing the previous position and adding the more recent position to iteratively calculate the current position of the AUV.

https://doi.org/10.1017/S0373463318000590 Published online by Cambridge University Press

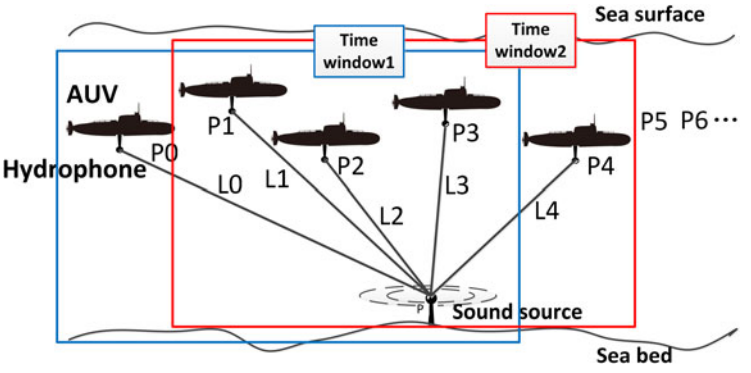

Figure 2. Time window model based on periodic movement.

3. ALGORITHM IMPLEMENTATION.

3.1. *Iterative updating of position based on moving virtual LBL windows.* Considering that the same algorithm is used to calculate the position of the AUV based on each window, we describe the calculation method for the AUV by taking the first window as an example.

The initial position of the AUV is denoted as $P_0\,(x_0, y_0, z_0)$ in the inertial coordinate system. From the above description, each new position of the AUV is obtained every *10Ts*, for example, $P_1\,(x_1, y_1, z_1)$, $P_2\,(x_2, y_2, z_2)$ and $P_3\,(x_3, y_3, z_3)$. The four positions form the first virtual LBL matrix window. The distances between position P_i $(i = 0, 1, 2)$ and P_3 in the three-axis direction (x, y, z) are defined as Δx_{3i}, Δy_{3i} and Δz_{3i} respectively; their values can be measured by dead reckoning using INS. P_i can be described by recent position P_3 as follows; its position is considered unknown and should be calculated:

$$\begin{cases} (x_0, y_0, z_0) = \left((x_3 - \Delta x_{30}), (y_3 - \Delta y_{30}), (z_3 - \Delta z_{30})\right) \\ (x_1, y_1, z_1) = \left((x_3 - \Delta x_{31}), (y_3 - \Delta y_{31}), (z_3 - \Delta z_{31})\right) \\ (x_2, y_2, z_2) = \left((x_3 - \Delta x_{32}), (y_3 - \Delta y_{32}), (z_3 - \Delta z_{32})\right) \end{cases} \tag{1}$$

Time difference τ_{3i} of the received signal at positions P_3 and P_i can be obtained through a cross-correlation operation. Two factors lead to the time difference. The first factor is the difference in geographic location (Δt_{3i}), and the second factor is the time interval of the sent signal, as indicated in Equation (2):

$$\Delta t_{3i} = \tau_{3i} - (30 - 10i)\,t, \quad (\mathrm{i} = 0, 1, 2) \tag{2}$$

https://doi.org/10.1017/S0373463318000590 Published online by Cambridge University Press

The sound propagation velocity underwater is assumed to be a constant value denoted as c, and three equations are established as follows:

$$\begin{cases} \Delta t_{30}c = \sqrt{(x_3-x)^2+(y_3-y)^2+(z_3-z)^2} \\ \quad -\sqrt{(x_0-x)^2+(y_0-y)^2+(z_0-z)^2} \\ \Delta t_{31}c = \sqrt{(x_3-x)^2+(y_3-y)^2+(z_3-z)^2} \\ \quad -\sqrt{(x_1-x)^2+(y_1-y)^2+(z_1-z)^2} \\ \Delta t_{32}c = \sqrt{(x_3-x)^2+(y_3-y)^2+(z_3-z)^2} \\ \quad -\sqrt{(x_2-x)^2+(y_2-y)^2+(z_2-z)^2} \end{cases} \tag{3}$$

(x_0, y_0, z_0), (x_1, y_1, z_1) and (x_2, y_2, z_2) can be expressed as expressions that contain (x_3, y_3, z_3) through Equation (1), and recent position P_3 (x_3, y_3, z_3) can be calculated by Equation (3). Subsequently, the recent geodetic coordinates can be obtained through the coordinate transformation of latitude and longitude.

The AUV coordinates in the geodetic coordinate and Earth rectangular coordinate systems are set as (λ, L, H) and (x, y, z), respectively. The formula for converting the geodetic coordinates into the Earth frame's rectangular coordinates is expressed as follows:

$$\begin{cases} x = (N+H)\, cosLcos\lambda \\ y = (N+H)cosLsin\lambda \\ z = [N\left(1-e^2\right)+H]sinL \end{cases}$$

where e is the first eccentricity and N is the radius of the unitary circle at latitude L.

$$N = a/\sqrt{\left(1-e^2 sin^2 L\right)}$$

where a is the long semi-axis of the Earth.

Therefore, the formula for converting the Earth's rectangular coordinates to geodetic coordinates is:

$$\begin{cases} \lambda = arctan\,(y/x) \\ L = \arctan\left(\dfrac{z+be_2^2 sin^3 U}{\sqrt{x^2+y^2}-ae^2 cos^3 U}\right) \\ H = \sqrt{x^2+y^2}/cosL - N \end{cases}$$

Among the coordinates, b is the short semi-axis of the Earth and e_2 is the second eccentricity, where $U = arctan\left(z/\sqrt{x^2+y^2}\sqrt{1-e^2}\right)$.

The first and second virtual LBL windows are used as examples to explain the iterative updating of the AUV position. The AUV continues to move and obtains the current position P_4 (x_4, y_4, z_4) after *10Ts* when the recent position P_3 (x_3, y_3, z_3) is obtained. P_0 (x_0, y_0, z_0) is removed from the window and P_4 is added in the new window with positions P_1, P_2 and P_3. The AUV updates the current position by using this method, which corrects the errors of the SINS.

https://doi.org/10.1017/S0373463318000590 Published online by Cambridge University Press

3.2. *Calculation of Time Difference of Arrival (TDOA).* A TDOA positioning method provides the sound source position by measuring the TDOA at different targets from the sound source. Given the difficulty of synchronising underwater signals, the time difference is easy to obtain through the cross-correlation processing of the received signals.

Assuming that the received signals at positions P_i and P_j are:

$$\begin{aligned} x_i &= a_i x\,(t-\tau_i) + n_i(t) \\ x_j &= a_j x\,(t-\tau_j) + n_j(t) \end{aligned} \tag{4}$$

where a_i and a_j are the attenuation coefficients of the acoustic signals that propagate underwater, $n_i(t)$ and $n_j(t)$ are the uncorrelated noise signals and τ_i, τ_j are the propagation times.

The cross-correlation function of $x_i(t)$ and $x_j(t)$ is:

$$R_{x_i x_j}(\tau) = E\left[x_i(t)\, x_j^*(t-\tau)\right] = \frac{1}{T-\tau}\int_{\tau}^{T} x_i(t)\, x_j(t-\tau)\, dt \tag{5}$$

where $\tau = \tau_j - \tau_i$ indicates the TDOA signals and T denotes the observation time. In theory, the peak of $R_{x_i x_j}$ corresponds to the time difference of $x_i(t)$ and $x_j(t)$, which is τ.

3.3. *Smooth Coherent Transformation (SCOT)-weighted generalised cross-correlation.* As a result of complicated underwater environments, refractions and reflections are common, and they are called multipath effects. Figure 3 shows a simplified multipath channel model of underwater acoustic propagation, in which only the direct propagation path (P_{iD},($i = 1, 2, \ldots$)), reflection propagation path of the sea surface (P_{iS},($i = 1, 2, \ldots$)) and reflection propagation path of the seabed (P_{iB},($i = 1, 2, \ldots$)) are considered. In addition, noise exists in the underwater environment, and includes the radiated noise of the AUV, oceanic reverberation and other factors that interfere with acoustic signals. This condition results in a number of similar peaks that correspond to different time differences. However, the positioning error is amplified after the time differences are multiplied by the speed of the acoustic propagation (Deng et al., 2009).

Mahdinejad and Seghaleh (2013) used a different weighted generalised cross-correlation method to calculate time delays and compared the experimental results in a reverberation room under an acoustic environment. They determined that the SCOT-weighted generalised cross-correlation algorithm obtains good results in acoustic signal processing and time delay estimation, and this method has better accuracy and precision than other methods. In this study, the SCOT-weighted generalised cross-correlation is used to make the relevant peaks prominent to effectively enhance the spectral component of the source signal in the received signal. Therefore, the signal-to-noise ratio is improved, and the cross-correlation function is enhanced. These improvements increase the accuracy of the estimation of the time difference.

The received signals of the hydrophone at positions P_i and P_j are transformed from the time domain into the frequency domain by using Fourier transformation:

$$\begin{aligned} F_{x_i}(\omega) &= \int_{-\infty}^{+\infty} x_i(t) e^{-j\omega t} dt \\ F_{x_j}(\omega) &= \int_{-\infty}^{+\infty} x_j(t) e^{-j\omega t} dt \end{aligned} \tag{6}$$

https://doi.org/10.1017/S0373463318000590 Published online by Cambridge University Press

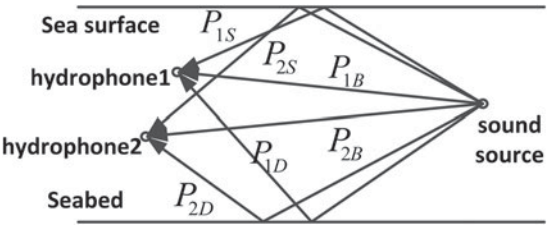

Figure 3. Simplified channel mode for underwater acoustic multipath propagation.

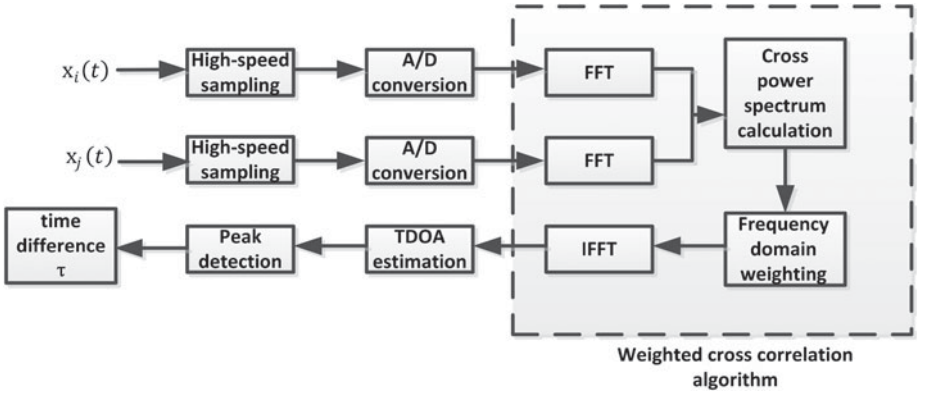

Figure 4. Flow chart of the SCOT frequency domain-weighted generalised cross-correlation algorithm.

The function of cross-power spectral density is obtained by the following equation:

$$G_{x_i x_j}(\omega) = F_{x_i}(\omega) F^*_{x_j}(\omega) \tag{7}$$

where $F^*_{x_j}(\omega)$ is the conjugate of $F_{x_j}(\omega)$.

According to the theorem of Wiener-Khinchin (Cohen, 1998), the relationship between the function of cross-power spectral density and cross correlation is:

$$R_{x_i x_j}(\tau) = \int_0^{\pi} G_{x_i x_j}(\omega) e^{-j\omega\tau} d\omega \tag{8}$$

To reduce the multipath interference and noise in the selection of correct correlation peaks, the received signals are processed by the above mentioned SCOT-weighted method. Signals x_i and x_j are passed through a pre-filter, and the SCOT-weighted general cross-correlation operation is performed on the pre-filtered signals. The cross-correlation function based on weighted function $\varphi_{x_i x_j}(\omega)$ in the frequency domain is:

$$R_{x_i x_j}(\tau) = \int_0^{\pi} \varphi_{x_i x_j}(\omega) G_{x_i x_j}(\omega) e^{-j\omega\tau} d\omega \tag{9}$$

The flow chart of the SCOT-weighted generalised cross correlation is shown in Figure 4.

The SCOT-weighted generalised cross-correlation function improves the proportion of effective spectra in the received signal, which suppresses the noise interference and

https://doi.org/10.1017/S0373463318000590 Published online by Cambridge University Press

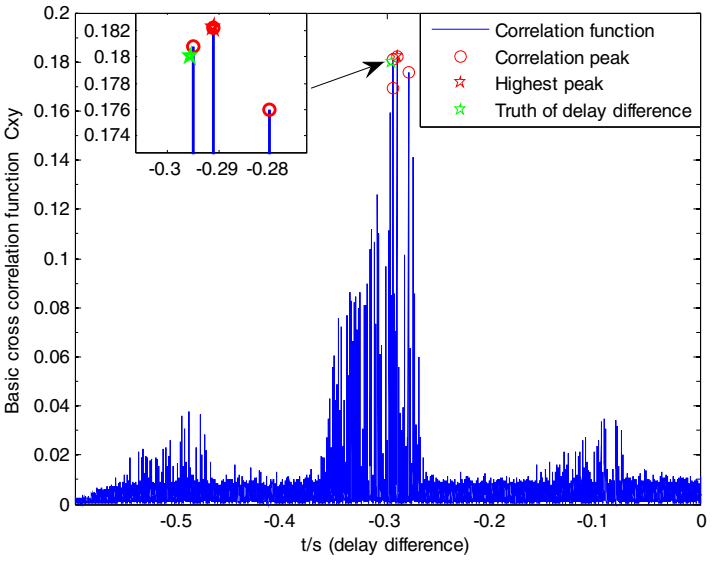

Figure 5. Basic cross-correlation function in simulation.

improves the accuracy of the estimated time difference. The abscissa value that corresponds to the maximum peak in the SCOT-weighted generalised cross-correlation function is the time difference τ.

4. SYSTEM SIMULATION AND SEMI-PHYSICAL EXPERIMENT.

4.1. *Simulation to verifying the validity of the SCOT weighted function.* The Bellhop model (Michael, 2011) is widely used in underwater acoustic channel simulation. This model is equally effective in channel analysis and modelling. It simulates underwater environment noise, multipath effects, and Doppler frequency shifts by introducing sound field data. It thus forms a real channel model and obtains various practical data, such as eigen line, impulse response, propagation loss and arrival time sequence of sound.

To verify the validity of the SCOT-weighted cross-correlation function in the frequency domain, we performed simulations and compare the method with traditional cross-correlation methods by establishing a propagation model of underwater acoustic signals using the Bellhop software. The sound source signal was selected as a type of amplitude modulation signal with a bandwidth of 40 kHz and a centre frequency of 22 kHz. The sound source was placed at a depth of 50 m, and two hydrophones were placed at a depth of 25 m underwater at different locations. The results of the two methods of cross-correlation functions are shown in Figures 5 and 6. The simulations were conducted three times, and the results are subsequently compared (Table 1).

Figures 5 and 6 and Table 1 show that the SCOT-weighted cross-correlation function in the frequency domain reduces the amplitude of pseudo-peaks near the ideal peak that corresponds to the time difference by eliminating the inference of multiple correlation peaks caused by the multipath propagation effect. The result reveals that the time difference estimated by this method is more accurate than that obtained by the traditional method.

https://doi.org/10.1017/S0373463318000590 Published online by Cambridge University Press

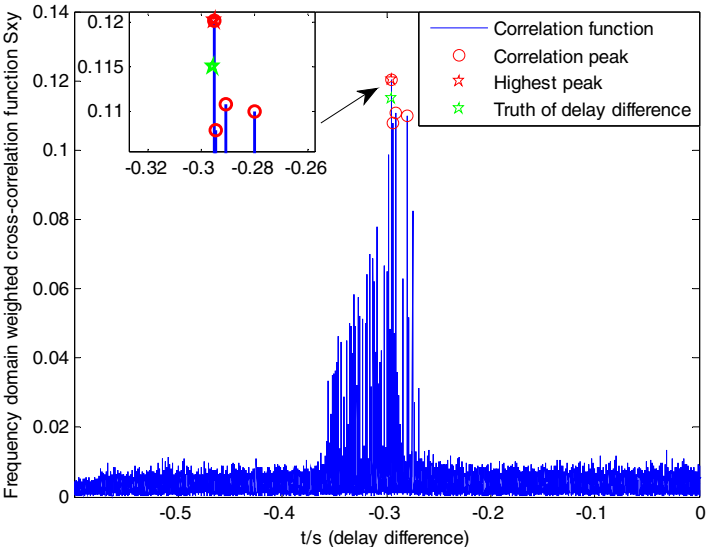

Figure 6. SCOT-weighted cross-correlation function in simulation.

Table 1. Comparisons of time difference errors in simulations.

Basic cross-correlation/s	SCOT-weighted cross-correlation/s
0·0044	0·0006
0·0068	0·0009
0·0105	0·0011

4.2. *Semi-physical experiment to verify the validity of the SCOT-weighted function.* To evaluate the performance of the above method, we conducted a semi-physical experiment involving an ultrasonic sound source and five receivers in an open space with low noise. The four receivers formed a square shape with a side length of 5 m, and the remaining receiver was placed in the centre of the square. The equipment layout is shown in Figure 7, and the experimental environment is shown in Figure 8.

The sound source signal is a type of pulse signal with a frequency of 40 kHz and a pulse width of 20 ms. The traditional cross-correlation and SCOT-weighted cross-correlation methods in the frequency domain were applied for the signals received by two receivers. The results are shown in Figures 9 and 10 and Table 2.

The result of the traditional cross-correlation method reveals several pseudo-peaks with similar peaks. By contrast, the SCOT-weighted cross-correlation method in the frequency domain effectively reduces all the amplitudes of the pseudo-peaks and attains the maximum peak. The results of the semi-physical experiment show that the SCOT-weighted cross-correlation method significantly enhances the real correlation peak and effectively estimates the time difference.

4.3. *Simulation of dynamic positioning.* A simulation was conducted to verify the dynamic positioning effect of the time window model based on periodic movement. A

https://doi.org/10.1017/S0373463318000590 Published online by Cambridge University Press

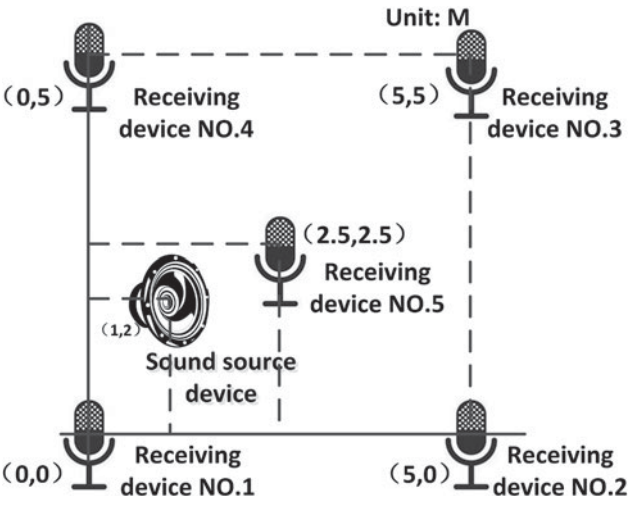

Figure 7. Equipment layout.

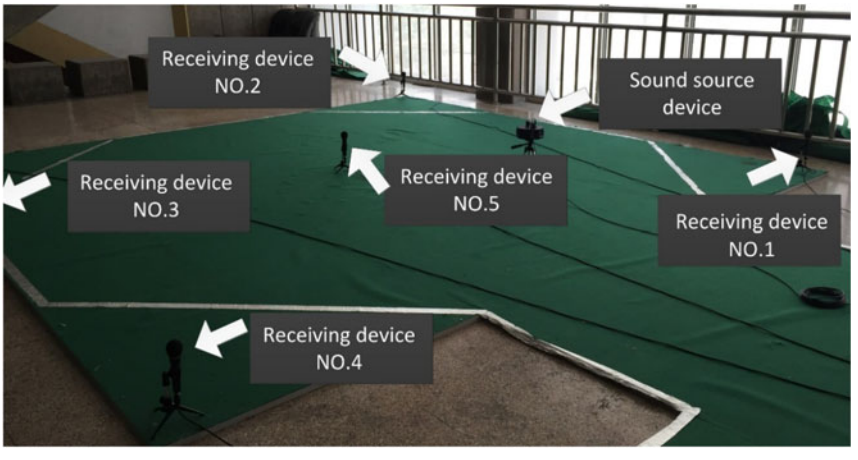

Figure 8. Experimental environment.

Table 2. Comparison of time difference errors in the semi-physical experiment.

Basic cross-correlation delay/s	SCOT-weighted cross correlation/s
0·0027	0·0011
0·0019	0·0008
0·0011	0·0004

Table 3. Rocking parameters of the AUV.

	Course	Pitch	Roll
Swing amplitude (°)	9	12	10
Rolling period (s)	8	10	6

https://doi.org/10.1017/S0373463318000590 Published online by Cambridge University Press

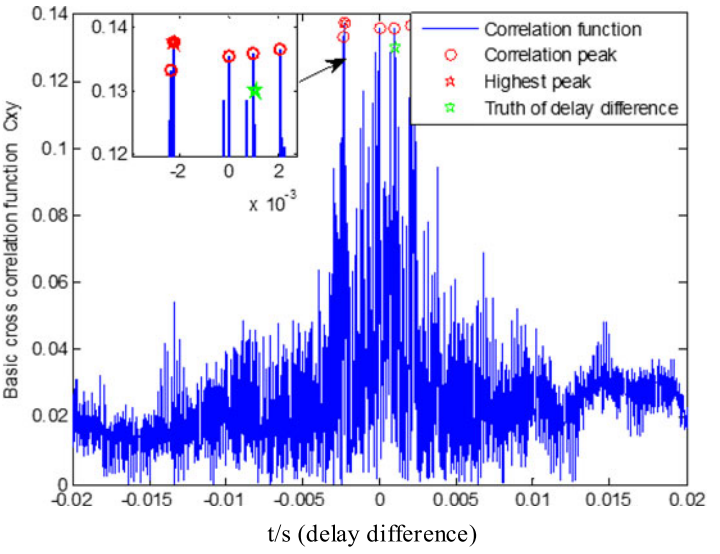

Figure 9. Semi-physical basic cross-correlation function graph.

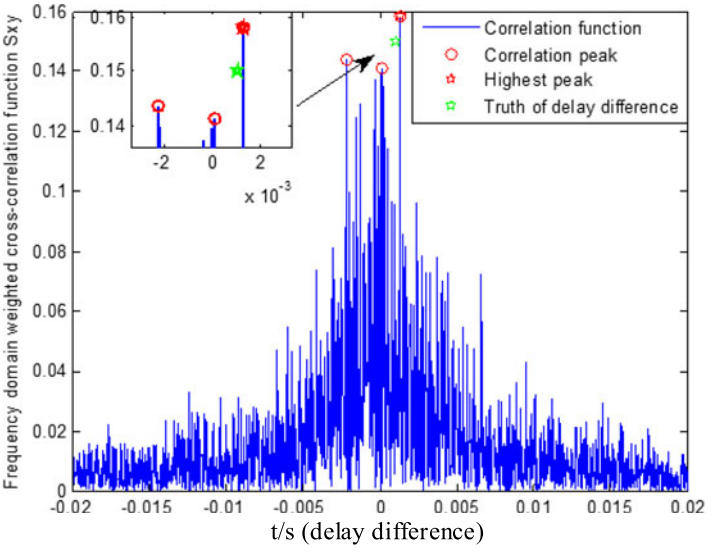

Figure 10. Semi-physical SCOT-weighted cross-correlation function graph.

single sound source was placed at a longitude of 120·01°, latitude of 40° and depth of 50 m. The sound source transmitted the pulse signal with a frequency of 0·025 Hz and a pulse width of 100 ms. The AUV moved along the northeast direction from its initial position of 119·995° longitude and 32·995° latitude at the speed of 1 m/s and depth of 25 m. The AUV swung in accordance with the three-axis sine model. The random and constant drifts of the gyroscopes were 0·05° h, and the random and constant biases of the accelerometers were 50 μg. The initial misalignment angles at the three axes were 1·5° and the period

https://doi.org/10.1017/S0373463318000590 Published online by Cambridge University Press

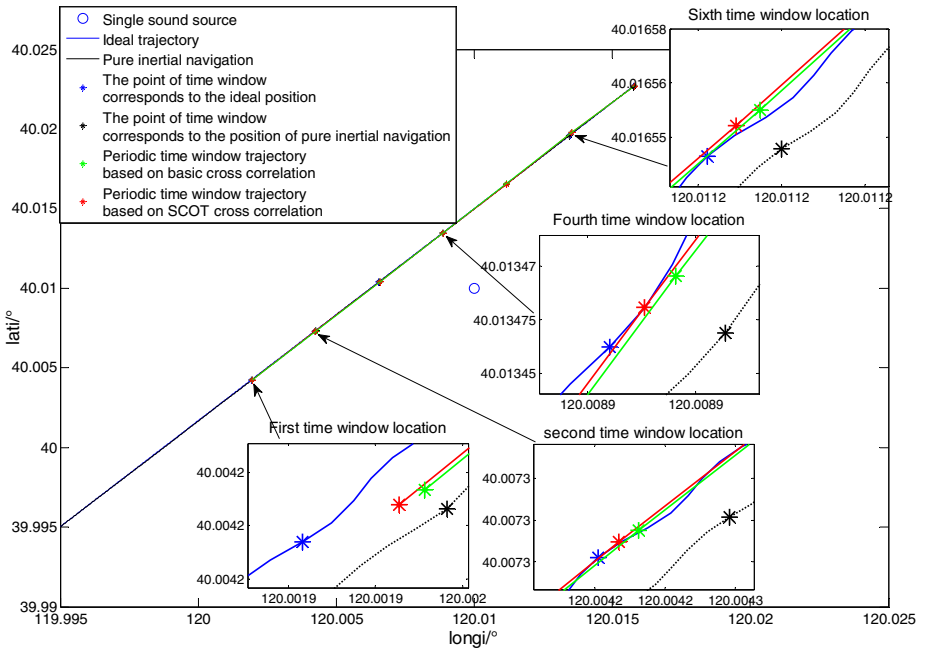

Figure 11. Comparison of two tracks with the ideal track.

Table 4. Comparison of pure inertia and acoustic cycle time window distance error.

Algorithm	Error of time window 1/m	Error of time window 2/m	Error of time window 3/m	Error of time window 4/m	Error of time window 5/m	Error of Time window 6/m
SINS	12·8299	13·6234	14·4311	14·9525	14·3763	15·0846
virtual LBL matrix window based on traditional cross correlation	2·2300	2·1788	2·5796	1·8128	1·9522	2·4984
virtual LBL matrix window based on SCOT-weighted cross-correlation function	1·9402	1·8872	1·6240	1·5874	1·7982	2·2245

of the time window was set as 400 s. The simulation time was 3,600 s. In the simulation, the AUV position was estimated only on the basis of the SINS for the first 1,200 s. The algorithm based on a virtual LBL matrix window was introduced to calculate the position for the remaining 2,400 s.

Three algorithms, namely the algorithms based on SINS with no LBL aiding, virtual LBL matrix window using traditional cross-correlation function and SCOT-weighted cross-correlation function in the frequency domain, are compared in Figure 11. Table 4 shows the positioning errors of the three algorithms. As shown in Figure 11 and Table 4, the position obtained by SINS significantly deviates from the real trajectory. This result indicates that the accumulated errors of inertial sensors have a considerable influence on the positioning accuracy of the AUV. In the initial stage of the algorithm based on the virtual LBL matrix

https://doi.org/10.1017/S0373463318000590 Published online by Cambridge University Press

window, the accuracy of the position is rapidly obtained to within 3 m. The positioning accuracy was improved as the number of iterations increased for the virtual LBL matrix window algorithm. The positioning result became accurate and reliable when the number of iterations reached four and five. Then, the positioning error gradually increases because the distance from the AUV to the sound source becomes large. Compared with the traditional cross-correlation function, the SCOT-weighted cross-correlation function in the frequency domain performs better and meets the high accuracy requirements of underwater vehicle navigation positioning.

5. CONCLUSION. Underwater acoustic positioning technologies have been investigated, and a virtual LBL matrix window method based on a SCOT-weighted cross-correlation function in the frequency domain proposed. A single hydrophone was installed at the bottom of the AUV, and a sound source was placed on the seabed. This set-up avoids the placement of a long and complex baseline array and reduces the cost. The proposed method also solves the problem of data communication and signal synchronisation underwater and enhances the concealment of AUVs. The experimental results show that the SCOT-weighted cross-correlation function calculates the time difference more accurately than the traditional cross-correlation function. Therefore, the algorithm based on a virtual LBL matrix window can provide precise underwater position at an accuracy of approximately 2 m.

ACKNOWLEDGEMENTS

The author would like to thank the support in part by the National Natural Science Foundation of China (Grant no. 51375088), Inertial Technology Key Lab Fund, the Fundamental Research Funds for the Central Universities (2242015R30031, 2242018K40065, 2242018K40066), the Foundation of Shanghai Key Laboratory of Navigation and Location Based Services.

REFERENCES

An, L., Chen, L. J. and Fang, S. L. (2013). Investigation on Correlation Peaks Ambiguity and Ambiguity Elimination Algorithm in Underwater Acoustic Passive Localization. *Journal of Electronics & Information Technology*, **35**(12), 2948–2953.

Barisic, M., Miskovic, N. and Vasilijevic, A. (2012). Fusing Hydroacoustic Absolute Position Fixes With AUV On-Board Dead Reckoning. *IFAC Proceedings Volumes*, **45**(22), 211–217.

Casalino, A. T. G., Simetti, E., Sperindè, A. and Torelli, S. (2014). Impact of LBL Calibration on the Accuracy of Underwater Localization. *IFAC Proceedings Volumes*, **47**(3), 3376–3381.

Choi, Y. H., Lee, J. W., Hong, S. H., Suh, J. H. and Kim, J. G. (2015). The development of the modular autonomous underwater navigation system based on OPRoS. *International Conference on Ubiquitous Robots and Ambient Intelligence*. IEEE, 625–628.

Cohen, L. (1998). The generalization of the Wiener-Khinchin theorem. *IEEE Signal Processing Letters,* **5**(11), 292–294.

Deng, A. D., Bao, Y. Q. and Zhao, L. (2009). Research on Time Delay Estimation Algorithm Based on Generalized Cross Correlation in Acoustic Emission Source Location. *Proceedings of the CSEE*, **29**(14), 86–92.

Donovan, G. T. (2012). Position Error Correction for an Autonomous Underwater Vehicle Inertial Navigation System (INS) Using a Particle Filter. *IEEE Journal of Oceanic Engineering*, **37**(3), 431–445.

Ferreira, B., Matos, A. and Cruz, N. (2010). Estimation approach for AUV navigation using a single acoustic beacon. *Sea Technology*, **51**(12), 54–59.

Ji, C. L., Zhang, N., Wang, H. H. and Zheng, C. E. (2014). Application of Kalman Filter in AUV Acoustic Navigation. *Applied Mechanics & Materials*, **525**, 695–701.

Ji, D. X., Song, W., Zhao, H. Y. and Liu, J. (2016). Deep Sea AUV Navigation Using Multiple Acoustic Beacons. *China Ocean Engineering (English Edition)*, **30**(2), 309–318.

Jiao, X. T., Li, J. C. and Men, L. J. (2013). Accuracy Analysis of Two TDOA Algorithms in Passive Underwater Acoustic Positioning. *Audio Engineering*, **37**(1), 73–75.

Lee, P. M., Huan, J. B., Choi, H. T. and Hong, S. W. (2005). An integrated navigation systems for underwater vehicles based on inertial sensors and pseudo LBL acoustic transponders. *Oceans. Washington, DC, USA, IEEE*, **1**, 555–562.

Mahdinejad, K. and Seghaleh, M. Z. (2013). Implementation of time delay estimation using different weighted generalized cross correlation in room acoustic environments. *Life Science Journal,* **10**(6S), 846–851.

Maki, T., Matsuda, T., Sakamaki, T., Ura, T. and Kojima, J. (2013). Navigation Method for Underwater Vehicles Based on Mutual Acoustical Positioning With a Single Seafloor Station. *IEEE Journal of Oceanic Engineering*, **38**(1), 167–177.

Michael, B. P. (2011). The BELLHOP Manual and User's Guide: PRELIMINARY DRAFT. *Heat, Light, and Sound Research, Inc.*

Miller, P. A., Farrell, J. A., Zhao, Y. Y. and Djapic, V. (2010). Autonomous underwater vehicle navigation. *IEEE Journal of Oceanic Engineering*, **35**(3), 663–678.

Morgado, M., Batista, P., Oliveira, P. and Silvestre, V. (2010). Position USBL/DVL sensor-based navigation filter in the presence of unknown ocean currents. *Automatica,* **47**(12), 2604–2614.

Ngatini, Apriliani, E. and Nurhadi, H. (2016). Ensemble and Fuzzy Kalman Filter for Position Estimation of an Autonomous Underwater Vehicle Based on Dynamical System of AUV Motion. *Expert Systems with Applications*, **68,** 29–35.

Paull, L., Saeedim S., Seto, M. and Li, H. (2014). AUV Navigation and Localization: A Review. *IEEE Journal of Oceanic Engineering*, **39**(1), 131–149.

Yu, P. and Wu, B. (2015). The optimal design of long baseline acoustic positioning array. *Ship Electronic Engineering*, **35**(5), 125–129.

Zhang, J. C., Han, Y. F., Zheng, C. and Sun, D. (2016a). Underwater target localization using long baseline positioning system. *Applied Acoustics*, **111**, 129–134.

Zhang, T., Chen, L. P. and Li, Y. (2015). AUV Underwater Positioning Algorithm Based on Interactive Assistance of SINS and LBL. *Sensors*, **16**(1), 42–64.

Zhang, T., Shi, H. F., Chen, L. P., Li, Y. and Tong, J. W. (2016b). AUV Positioning Method Based on Tightly Coupled SINS/LBL for Underwater Acoustic Multipath Propagation. *Sensors*, **16**(3), 357–373.

Zhang, T., Xu, X., Li, Y. and Gong, S. P. (2013). AUV fault tolerant navigation technology based on ins and underwater acoustic assistance system. *Chinese Journal of Inertial Technology*, **21**(4), 512–516.

Zhong, S., Xia, W. and He, Z. S. (2015). Multipath Time Delay Estimation Based on Gibbs Sampling under Incoherent Reception Environment. *IEICE Transactions on Fundamentals of Electronics Communications & Computer Sciences,* **E98.A**(6), 1300–1304.